JOURNAL OF Applied Polymer SCIENCE

Formation and Evolution of the Carbon Black Network in Polyethylene/Carbon Black Composites: Rheology and Conductivity Properties

Danqi Ren, Shaodi Zheng, Feng Wu, Wei Yang, Zhengying Liu, Mingbo Yang

College of Polymer Science and Engineering, State Key Laboratory of Polymer Materials Engineering, Sichuan University, Chengdu 610065, Sichuan, People's Republic of China

Correspondence to: Z. Liu (E-mail: liuzhying@scu.edu.cn)

ABSTRACT: We report a detailed investigation on the effect of carbon black (CB) morphology on network formation and evolution in high-density polyethylene/CB composites. There were three types of networks in our study, the electrical network in the solid state and the electrical and rheological networks in the melt state. The evolution of the network in the polymer melt was traced by simultaneous electrical resistivity (R) and dynamic rheology testing. An oscillation strain sweep was used to investigate the network stability with a large strain. We found that with high-structure CB with a branched morphology, it was easier to form a filler–polymer or filler–filler network than with low-structure CB with a spherical morphology in the composite melt. The high-structure CB network was more stable with a large strain compared to the low-structure one. Meanwhile, the low-structure CB aggregates had stronger capability of movement and re-aggregation in the polymer melt. © 2013 Wiley Periodicals, Inc. J. Appl. Polym. Sci. **2014**, *131*, 39953.

KEYWORDS: nanoparticles; nanowires and nanocrystals; properties and characterization; rheology

Received 5 March 2013; accepted 9 September 2013

DOI: 10.1002/app.39953

INTRODUCTION

Carbon black (CB) has been widely used as a conductive particle and in filled isolating polymer systems. Studies on it never stop because CB is relatively inexpensive and easy to obtain and shows good performance in terms of its high electrical conductivity.[1–5] In general, filled polymers exhibit a drastic transition from an electric insulator to a conductor at critical filler loading. This transition is called *percolation,* and the critical fillers loading is known as the *electrical percolation threshold* ($m_{c\delta}$). The percolation is due to the formation of a continuous CB conductive network throughout the polymer matrix. The electrical properties of conductive polymer composites (CPCs) with CB as the conductive filler are greatly affected by the CB properties, including its aggregate structure, particle size, specific surface area, and surface chemistry. Among these factors, the structure of CB is the most important factor influencing the stability and efficiency of the conducting network. There have been many reports on the effects of the CB structure on the electrical conductivity of CPCs.[6–9] It is widely recognized that composites filled with high-structure CB can obtain a higher conductivity at the same CB loading.[10]

Many former theories and modeling focused on the conducting network in the polymer solid state.[11–13] Nevertheless, the final morphology of the composite is usually determined by the melt processing and the cooling conditions. It is very important to understand the development of the conducting network in the polymer melt state. Fillers will markedly impact the viscoelasticity of bulk polymers. Dynamic rheology is widely used to study the dynamics and microstructure evolution of the composites. The dynamic rheological properties of polymer/filler composites are very sensitive to the content, dispersion state, and properties of filler particles. The storage modulus (G'), loss modulus (G''), and loss tangent ($\tan\delta$) can be used to characterize the different rheological networks formed in the composite melts. The phenomenon that the composite melt behavior translates from liquidlike to solidlike at low frequency (ω) reveals the existence of a rheological network.

When distinguishing the difference between electrical and rheological networks in the polymer melt, we should consider the complementary size scales of the components in a composite. Three types of networks may be discussed: the entangled network in the bulk polymer and the polymer–filler and filler–filler networks in the composite.[14] At low filler loadings, the composite melt behaves similarly to a neat polymer and shows a liquidlike behavior. The relationships between G', G'', and ω in the terminal region follow: $G' \approx \omega^2$ and $G'' \approx \omega^1$. With increasing filler loading, the interaction zones between the bulk polymer

and the filler overlap continuously. A network could be formed between the polymer and filler; this leads to concentration-dependent changes in the filler viscoelastic properties at long timescales. This polymer–filler network is often referred to as a *percolated rheological network*. At higher filler concentrations, the fillers form an electrically connected network.[14] The approximate threshold concentration for this network is tied to changes in the electrical properties and is also modeled as percolation. In general, three types of networks (polymer–polymer, polymer–filler, and filler–filler) have been used to explain the rheological behavior of filled polymers. However, the conducting network is mainly filler–filler interaction. With an electronic-transport mechanism defining this network, the fillers may not be strictly touching, but the interparticle spacing should be less than the distance needed for electron hopping or tunneling.[15]

Combining conductivity and rheological measurements provides new experimental information for better understanding the agglomeration kinetics of particles in polymer melts, so we can survey the evolution of electrical and rheological networks at the same time.[1–3,15–17] Cao et al.[1,2] studied the thermally induced dynamic percolation for both resistivity and G' as a function of the annealing time in high-density polyethylene (HDPE)/CB composites and polystyrene/CB composites. The percolation times were calculated, and the effects of the temperature and filler volume fraction on the percolation times of the resistivity and G' were reported. The results indicate that the interfacial tension between the polymer matrix and CB played a crucial role in driving CB to aggregate. Skipa and coworkers[16,17] considered the destruction and buildup of the carbon nanotube (CNT) network in polymer melts. They found that for melts with well-dispersed CNTs, a shear-induced insulator–conductor transition was obtained; this was explained by the agglomeration of CNTs under steady shear and the formation of an electrical conducting network of interconnected agglomerates. Huang et al.[15] investigated the dynamic electrical and rheological percolations in isotactic polypropylene (iPP)/CB and suggested that rheological percolation was more difficult to achieve than electrical percolation in the iPP/CB composites. Simultaneous measurement is a good way to study the electrically conductive and rheological networks at the same time.

To our knowledge, the influence of the CB fractal structure on the network formation and evolution in polymer/CB composites has not been particularly investigated yet. However, CBs with different fractal structures can build various networks in the polymer matrix, and this is often ignored.

In our previous study, we found that a high-structure CB could build an effective conducting network at a low filler contents compared to a low-structure one because of its branched morphology.[18] In this study, we focused on the influence of the CB structure on the electrical and rheological network formation and evolution. The electrical percolation and the rheological percolation of the HDPE-based composites filled with CB with different structures were investigated. An oscillation strain sweep was used to investigate the network stability with a large strain. The electrical and rheological network evolution was traced by simultaneous electrical resistance and dynamic rheology testing. We were the first ones to research the CB structure through dynamic rheology. The results of this study will be very helpful in the design of electrical functional materials, such as highly conductive performance materials and positive-temperature-coefficient materials.

EXPERIMENTAL

Materials and Sample Preparation

A commercial HDPE (HDPE 2911, with a melt flow rate of 20 g/10 min at 190°C/2.16 kg, supplied by Lanzhou Petroleum Chemical Co, Ltd., China) was used as the matrix. The types and properties of CB fillers used in this study are given in Table I. The three types of CB used in this study were supplied by Cabot Corp. The HDPE/CB composites were prepared by melt mixing in a Haake mixer (XSS-300, Shanghai, China) at a temperature of 190°C and at 60 rpm for 10 min. The mixtures from Haake were compressed into a plate with a thickness of 2 mm and then cut to dimensions of 10 × 30 × 2 mm^2 for electrical conductivity characterization. In the meanwhile, the samples for rheological characterization were compressed in a mold with a thickness of 1.5 mm and a diameter of 2.5 mm. The hot press was completed under a pressure of 10 MPa at 190°C for 5 min. Then, the testing samples were cooled to room temperature under the same pressure. Before we performed the measurements, all of the composites sheets were rested overnight to release stress.

Characterization

Electrical Conductivity Characterization. A two-probe method was used to obtain the room-temperature volume resistivity of the samples with an electrometer (Keithley 6517B) when the resistivity of them were lower than 10^8 Ω cm. At both ends of the sample, the surface (10 × 2 mm^2) was put into contact with the copper electrodes, which were painted with silver to ensure good contact, although a high-resistivity meter (ZC360) was used for the samples (100 × 100 × 2 mm^3) with higher resistivity (>10^8 Ω cm).

Morphological Observation. The specimens were fractured after they were frozen in liquid nitrogen for 1 h. The fracture surfaces were covered with a layer of gold to make them

Table I. Types and Properties of the CBs Used in the Experiments

Structure	Commercial name	DBP volume (mL/100 g)	Mean particle size (nm)	Specific surface area (m^2/g)
High	BP2000	330	15	1475
Medium	VXC-72	178	30	254
Low	VXC-68	123	25	68

conductive, and we then observed them with an FEI INSPECT F scanning electron microscope.

Rheological Characterization. A stress-controlled rheometer (AR 2000ex, TA Instruments, Ltd.) equipped with parallel-plate geometry (diameter = 25 mm) was used. The tested temperature was 160°C, and the gap between the plates was fixed at 1.2 mm. A dynamic ω sweep was conducted from 0.063 to 502 rad/s under a 0.1% strain in the linearity region. The strain sweep had a strain range of 0.01–200% and an ω of 6.28 rad/s. We fulfilled the combined rheological and electrical measurements by setting the parallel plates as electrodes and using a Keithley 6517B to measure the resistance of the composite melts between the plates. A voltage of 0.5 V was used.

RESULT AND DISCUSSION

CB primary aggregates are composed of primary particles. The aggregate size and shape and the number of primary particles per aggregate determine the structure of CB.[10,19] The most commonly used parameter to describe CB structure is the amount of dibutyl phthalate (DBP) absorbed per 100 g of CB. A greater amount of DBP indicates a higher CB structure. As shown in Table I, BP2000 is a typical high-structure CB[6,20] with DBP volume = 330 ml/100 g and VXC-72 is a comparative medium-structure CB with DBP volume = 178 ml/100 g, meanwhile the DBP absorption of VXC-68 is lowest in all of used CB (DBP volume = 123ml/100 g) in this study. The primary aggregate morphologies of the differently structured CB can be found in our previous publication.[18]

Effect of the CB Structure on the Network Formation in the Solid State

Figure 1 shows the room-temperature resistivity as a function of the filler content for the HDPE/CB composite. As shown in Figure 1, the room-temperature resistivity of the HDPE/CB composite decreased sharply with increasing CB content when the CB content was lower than the percolation threshold. A power law relation was used to further describe the electrical conductivity percolation:

$$R \propto (m - m_{c\delta})^t \quad (1)$$

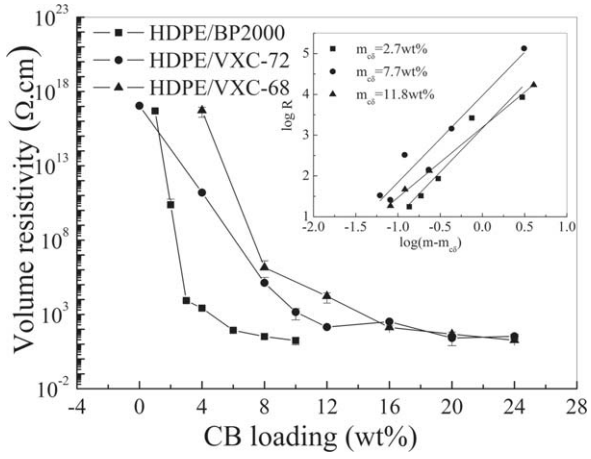

Figure 1. Volume resistivity of the HDPE/CB composites filled with different kinds of CB as a function of the CB loading. The inset represents the fits to the percolation law.

where R is the electrical resistivity, m is the mass fraction of CB, and t is the critical exponent. The CB structure impacted the threshold behavior of the CPCs, as shown in inset of Figure 1. The HDPE/BP2000 composite had the smallest $m_{c\delta}$ ($m_{c\delta} = 2.7$ wt %), which was far lower than that of the HDPE/VXC-72 ($m_{c\delta} = 7.7$ wt %) and HDPE/VXC-68 ($m_{c\delta} = 11.8$ wt %) composites. It is widely recognized that the percolation threshold value is a remarkable reflection of the ability of the particles to build a conducting network in CPCs. Generally speaking, a high-structure CB with a branched morphology has a stronger tendency to build an effective network in the matrix, so the composite filled with BP2000 had a lower percolation threshold.[4,5]

Scanning electron microscopy (SEM) was used to obtain direct information about the conductive network formed by the differently structured CBs. The image in Figure 2(a) indicates that the high-structure CB was well dispersed in the 0.1–0.3-μm aggregate state in the polymer matrix. The aggregates interconnected into a well-defined network even when the particle loading was 4 wt %. The images in Figure 2(b,c) indicate that the medium- and low-structure CBs dispersed in the host polymer as big CB aggregates (ca. 0.5 μm); this means that it was difficult to form a conductive network when the CB content was 4 wt %. The SEM images show that compared to the high-structure CB, with the medium- and low-structure CBs, it was easier to form a big cluster in the polymer melt; this completely explains the higher percolation thresholds in the medium- and low-structure CB-filled composites.

Effect of the CB Structure on the Rheological Network Formation in the Composite Melts

The terminal region of log G' (or log G'') versus log ω plots had a distinct yield behavior in all of the CB-filled systems. However, G' was a more sensitive rheological function to the structural changes of the composites than G''.

The ω–G' relationships of the composites containing different kinds of CB are shown as Figure 3. With increasing CB content, G' increased because the CB clusters reduced the mobility of the polymer chain and increased the melt's resistance to flow.[21] With further increases in the CB content, a rubbery plateau, which suggested a solidlike behavior of the composite melt, was observed at low ω. As shown in Figure 3(a), G' of the HDPE/BP2000 composite containing 2 wt % CB did not show a low-ω plateau. This result means that there were no interactions among the CB particles and no significant interactions between the particles and the polymer matrix. As the CB fraction increased, the slope of log G' versus log ω plots in the terminal region for the HDPE/CB composites become much lower than 2. This suggested that the composite exhibited a transformation from liquidlike to solidlike states because of filler–polymer or filler–filler network formation. For the HDPE/VXC-72 [Figure 3(b)] and HDPE/VXC-68 [Figure 3(c)] systems, the rubbery plateau of G' did not appear until the content of CB reached 8 wt %. From Figure 3, we concluded that the CB structure strongly affected the viscoelastic properties of the composites. BP2000 had stronger filler–polymer and filler–filler interactions than VXC-72 and VXC-68 because of its high specific surface

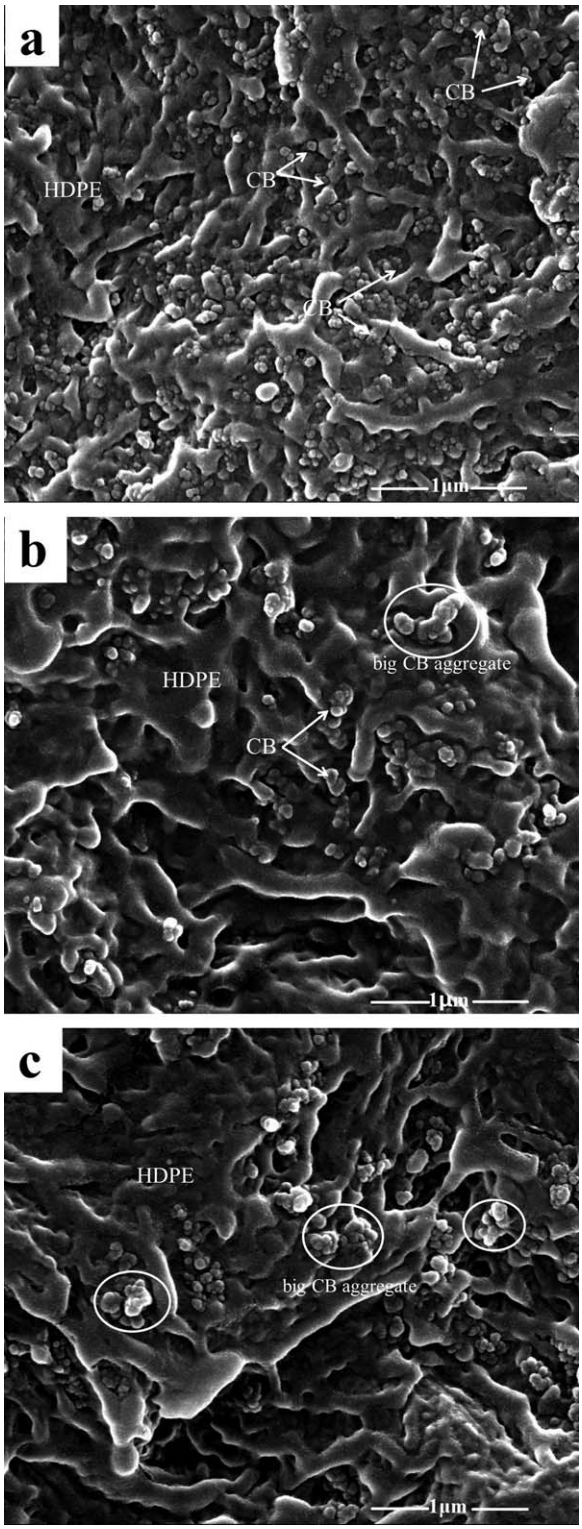

Figure 2. SEM images of the HDPE/CB composites: (a) HDPE/BP2000, (b) HDPE/VXC-72, and (c) HDPE/VXC-68. The CB loading was 4 wt %.

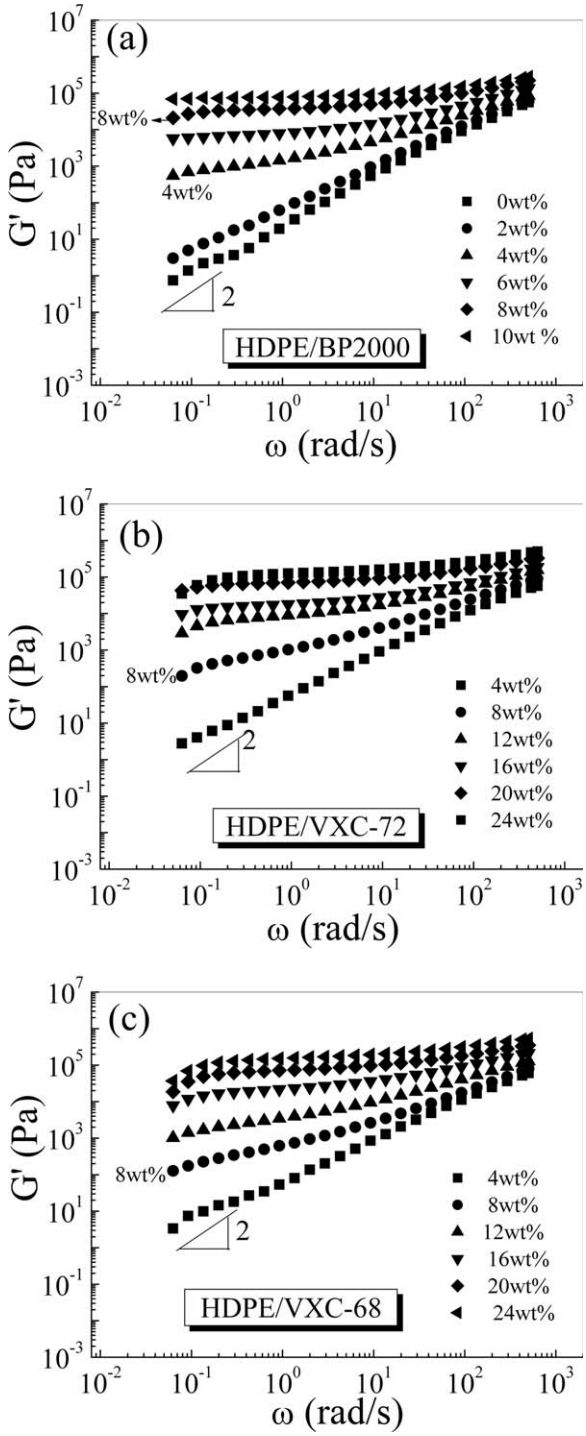

Figure 3. ω dependence of G' for the HDPE/CB composites with various CB structures: (a) HDPE/BP2000, (b) HDPE/VXC-72, and (c) HDPE/VXC-68. The rheological experiments were performed at 160°C and a 0.1% strain.

area. Thus, the HDPE/BP2000 composite appeared to have a rubbery plateau at lower CB loadings in contrast to the HDPE/VXC-72 and HDPE/VXC-68 composites. When considering all of the composites filled with 8 wt % CB [Figure 3(a–c)], we observed that the composite with high-structure CB had the smallest low-ω slope of G' and an obvious plateau in the terminal region. The HDPE/VXC-72 and HDPE/VXC-68 composites exhibited weak nonterminal rheological behavior; this means that the molecular motion in these composites was more like that of pure HDPE and the flow of the polymer chains was not

greatly influenced by the low-structure CB because of the loose aggregation formed by this kind of particle.

Quantitative interpretation of the rheological features of G' versus m plots for the three types of CB-filled systems is described by the power law:[11]

$$G' \propto \left(m - m_{cG'}\right)^{\beta_{G'}} \quad (2)$$

where $m_{cG'}$ is the threshold of the rheological percolation and $\beta_{G'}$ is the critical exponent. To further study the effects of the CB structure on the rheology of the composites, $m_{cG'}$ and $\beta_{G'}$ of the HDPE/CB composites were evaluated by the fitting of the experimental data at $\omega = 0.092$ rad/s with eq. (2). The $m_{cG'}$ values for the HDPE/BP2000, HDPE/VXC-72, and HDPE/VXC-68 composites were 3.1, 6.0, and 10.4 wt %, respectively (Figure 4).

It is worth noting that the electrical and rheological percolations can be different.[11,15,22] Du et al.[11] found that $m_{cG'}$ was smaller than the electrical percolation in poly(methyl methacrylate)/single-walled CNT composites. Huang et al.[15] suggested that the rheological percolation was more difficult to achieve than the electrical percolation in iPP/CB composites. Pötschke et al.[22] demonstrated that the two percolations could be different, as the rheological percolation strongly depends on the measurement temperature. The results in these studies indicate that although the rheological and electrical percolations were not consistent and involved different mechanisms, both of them reflected the influence of the CB structure on network formation in the polymer matrix.

The ω dependence of tan δ is depicted in Figure 5. The higher the CB loadings were, the smaller the value of tan δ was in the low-ω region. At the same time, tan δ was nearly independent of ω. This indicated an increase in the solid properties of the composite systems.[23] It is obvious from Figure 5(a) that the addition of 4 wt % BP2000 produced a notable decrease in the tan δ value, and the slope of the curve changes from negative to positive in the low-ω region. This solidlike rheological behavior was attributed to the filler–polymer network in composite. When the BP2000 loading increased to 6 wt %, the plot of tan δ versus ω began to change from a linear to an arc form, and a minimum point (the point that the slope of the tan δ curve changed from negative to positive) of tan δ appeared. The existence of the tan δ minimum point was considered to be a critical relaxation behavior involved in the high-order structure within the polymer matrix, which was related to the existence of the interparticle network.[24–26] However, for the HDPE/VXC-72 and HDPE/VXC-68 composites [Figure 5(b,c)], the tan δ minimum point did not appear until the CB loadings reached 8 wt %. What is more, the corresponding ωs of the HDPE/VXC-72 and HDPE/VXC-68 composites in the minimum point were higher than that of the HDPE/BP2000 composite. The result shows again that the ω dependence of tan δ could describe the network constructed by differently structured CBs.

Dynamic rheology is a reliable way to research the effect of the CB structure on the network formation in the polymer matrix because G' and tan δ are sensitive to the content and properties of the fillers. Although the rheological percolation was more complex than the conductive percolation because the two networks follow different mechanisms, we found that the HDPE/BP2000 composite had a lower $m_{cG'}$. High-structure CB, which had a branched morphology, formed intensive networks (filler–filler and filler–polymer networks) more easily in the matrix.

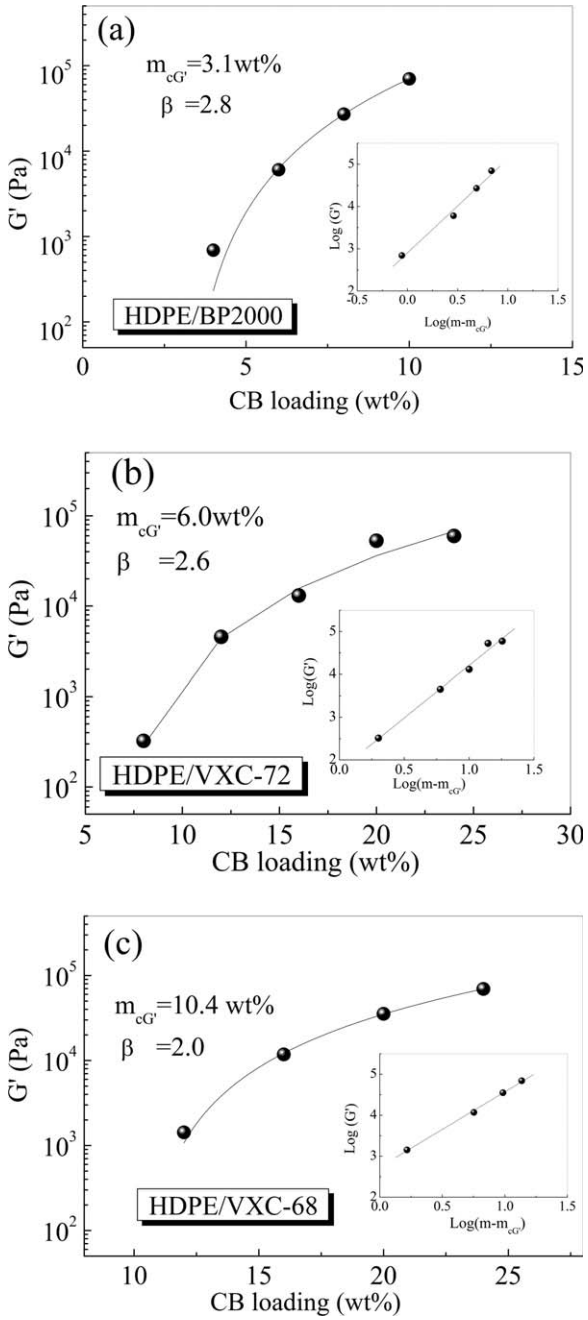

Figure 4. G' of the HDPE/CB composites as a function of the CB loading at a fixed ω of 0.092 rad/s: (a) HDPE/BP2000, (b) HDPE/VXC-72, and (c) HDPE/VXC-68. The insets show the log–log plots of G' versus the reduced mass fraction.

Effect of the CB Structure on the Network Stability

The Payne effect of composites is one nonlinear behavior and is related to the fractal structure of nanoparticles.[27] For a specific ω, G' decreases from a linear plateau to a lower value at a high

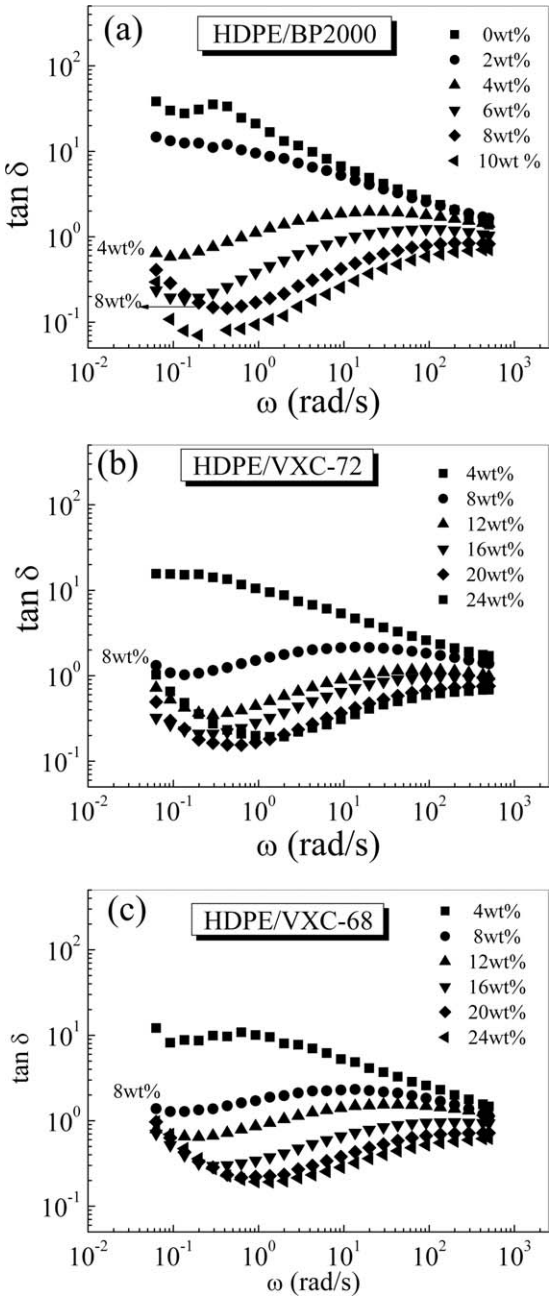

Figure 5. ω dependence of tan δ for the HDPE/CB composites: (a) HDPE/BP2000, (b) HDPE/VXC-72, and (c) HDPE/VXC-68. Rheology was performed at 160°C and a 0.1% strain.

amplitude of deformation. The nonlinear behaviors of composites are associated with chain disentanglements and the breakdown of the particle aggregate structure. Furthermore, as a consequence of the Payne effect, the *limit of the linearity* (γ_c), defined as the maximum strain in the linear region, decreases with increasing content of particles according to the following power law:

$$\gamma_c \propto \phi^{-v} \tag{3}$$

where &phis; is the mass fraction of fillers and v is the exponent relative to the particle properties. Actually, there have been many studies paying attention to the exponent. Rueb and Zukoski[28] observed that v strongly depended on the interparticle force and obtained values of v ranging from 0.7 to 4.0. According Zhu and Sternstein,[29,30] for hydrophobic and hydrophilic silica, the v values were 2.4 and 3.0, respectively. Bahloul et al.[27] reported that in PP/TiO_2 nanocomposites, v was 0.75. In addition, a power law close to γ_c ∝ &phis;$^{-1}$ was reported (for aggregates of spherical primary particles[31–33]). The results of the strain sweep supported the concept that the modulus and the strain γ_c were related to the fraction and fractal structure of the particles.[27,32]

As shown in Figure 6(a–c), for the HDPE/BP2000, HDPE/VXC-72, and HDPE/VXC-68 composites, the v values were 1.61, 1.89, and 2.24, respectively (Figure 6, inset). It seems that a tight filler–filler or filler–polymer network could be built by a high-structure CB in the polymer matrix, and the HDPE/BP2000 composite corresponded to a lower v value. However, as shown by the high v values of the HDPE/VXC-72 and HDPE/VXC-68 composites, weak filler–filler or filler–polymer interactions were obtained. The results indicate that the rheological network constructed by the high-structure CB was more stable with the large strain compared to the low-structure one.

Electrical and Rheological Network Evolution in the Composite Melts

To achieve further understanding of the influence of the CB structure on the electrical and rheological network evolution in the polymer melts, the HDPE/BP2000 and HDPE/VXC-68 composites were used and investigated by simultaneous time-resolved measurements of the electrical conductivity and rheological properties. The CB loadings of the HDPE/BP2000 and HDPE/VXC-68 composites were both above the electrical percolation and $m_{cG'}$. Figure 7 shows the time-dependent relative resistivity ($R' = R/R_0$, where R_0 is the initial resistivity of the composite melts and R is the test resistivity) during annealing in the rheometer. HDPE/BP2000 and HDPE/VXC-68 showed different trends in the early stage (0–1000 s). For the HDPE/VXC-68 composite, R' decreased more sharply with time than for the HDPE/BP2000 composite. After a certain time, the filler network reached its steady state, which was characterized by a constant R' in the composite melt. The HDPE/VXC-68 composite needed a longer time to reach its resistivity constant than did the HDPE/BP2000 composite. The result shows that the low-structure CB aggregates had a stronger capability of movement and reaggregation in the polymer melt. They also suggest that the initial network formed by the low-structure CB was inefficient.

The R' evolutions in Figure 7 reflect the evolution of the conductive network in the polymer melts. The decrease in R' shows the fact that the CB clusters reaggregated and reconstructed the new electrical network. Meanwhile, the low-structure CB cluster showed a stronger tendency to form a better conductive network with increasing time. The excess interfacial energy of the conductive particles was considerably high. CB aggregates in the melt tended to agglomerate to reduce excess interfacial energy;[1,34,35] this was accelerated because of the decrease in the viscosity of the melt. The driving force for the agglomeration might have been the strong dispersive interaction between the

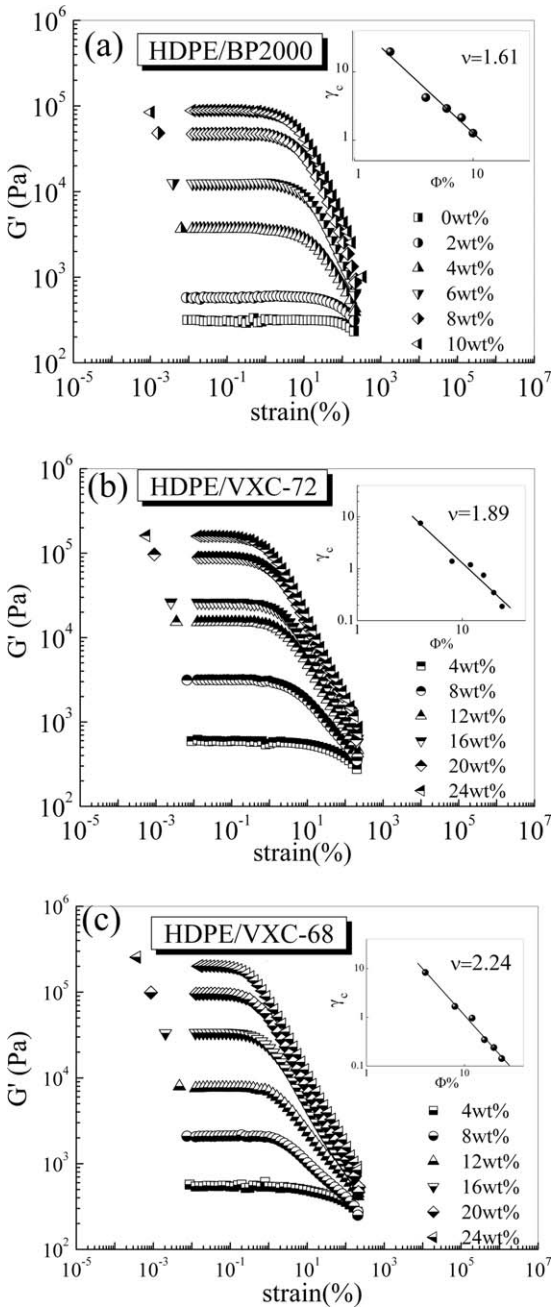

Figure 6. Strain dependence of G' for HDPE filled with different CBs at 160°C: (a) HDPE/BP2000, (b) HDPE/VXC-72, and (c) HDPE/VXC-68. The insets show the plots of the power law for γ_c.

CB and the matrix and the depletion interaction between adjacent CB aggregates.[36]

The addition of CB to the polymers led to dramatic changes in the viscoelasticity of the melt. Figure 8(a) shows the time-dependent relative G'/G'_0 (where G'_0 is the initial storage modulus of the composites and G' is the test storage modulus) during annealing in the rheometer. As shown in Figure 8(a), G'/G'_0 of the HDPE/VXC-68 composite was clearly higher than that of the HDPE/BP2000 and composites. The marked modulus increase with time in the HDPE/VXC-68 composite reflected

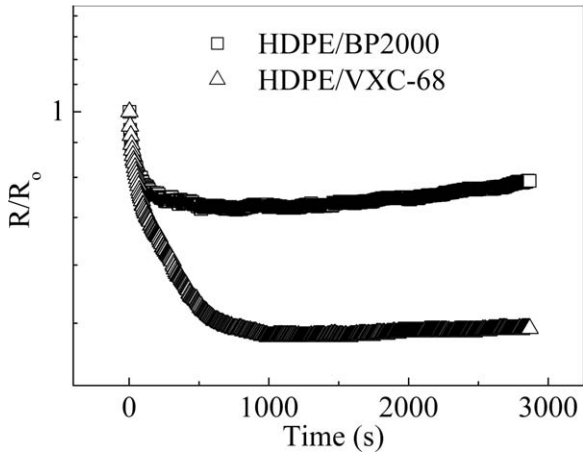

Figure 7. Time dependence of R' for the HDPE/BP2000 (4 wt %) and HDPE/VXC-68 (12 wt %) composites with simultaneous measurement. ω was 6.28 rad/s, and the strain was 0.1%.

that greater particle aggregate led to the formation of a combined network.[2]

In all of the rotary rheometer measurements, the samples were initially squeezed in place before the measurements were initiated. When the set-point gap (in our study, the gap value was

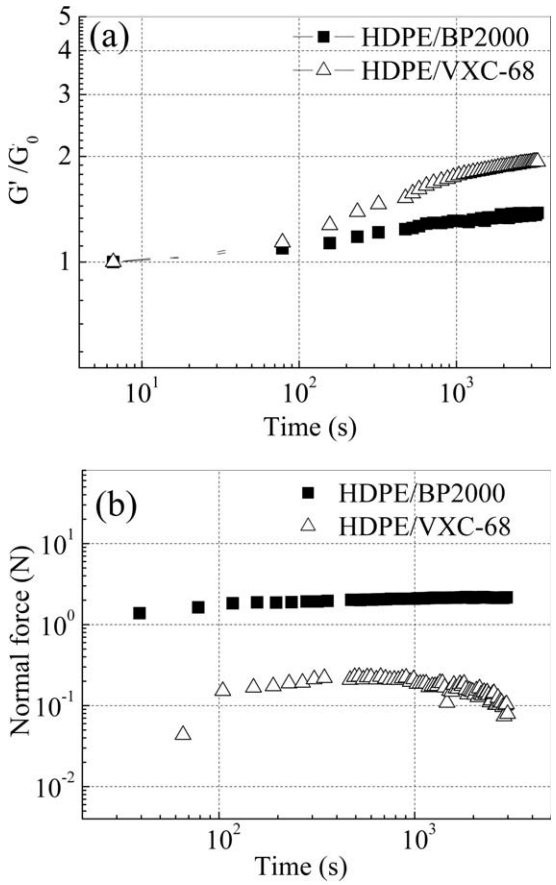

Figure 8. Time dependence of (a) G' and (b) the normal force for the HDPE/BP2000 (4 wt %) and HDPE/VXC-68 (12 wt %) composites with simultaneous measurements.

1200 μm) of the instrument was reached, the squeezing then stopped. After cessation of sample deformation, the stress induced by squeezing should have relaxed. The time relaxation process required could be recorded by the decay of normal force with time. What is more, the critical time is relative to the network relaxation in polymer melts.[37,38] Figure 8(b) shows the decay of the squeezing stress (represented by the normal force) with time in a log–log plot for the HDPE/CB composites. It is evident from Figure 8(b) that for the HDPE/BP2000 composite, the squeezing stress remained relatively constant on the timescales of our rheological experiments; this meant that the composite was more like a solidlike paste or a gel than a fluid in its viscoelastic response. Meanwhile, for the HDPE/VXC-68 composites, the squeezing stress decayed with time; this indicated that the squeezing stress exhibited an elastic relaxation. The decay in squeezing stress after the cessation of squeezing deformation was a consequence of the filler network relaxation within the polymer matrix. It seemed that the network built by high-structure CB is more stable than the network built by low-structure one.

Model of Network Formation and Evolution

It is important to clarify how the filler network develops during melting to better understand the effects of the CB structure on the network formation and evolution. A simplified model for the networks of two different CBs is shown in Figure 9. As shown in Figure 9(a), the network constructed by the high-structure CB was steady and almost did not change with melt annealing. This can be clarified as follows. First, the branched morphology of the filler facilitated network formation in the composites, so a lower content of CB was enough to form the network. Second, with a bigger specific surface area, more polymer chains were absorbed on the surface of the high-structure CB; this made the polymer–filler network more rigid. Therefore, the filler-bridged polymer network was not sensitive to the strain and thermal expansion of the polymer matrix. In our previous study on iPP/CB composites, a model was proposed that the high-structure CB could attach more polymer chains on itself.[4,5,15] However, for low-structure CB [Figure 9(b)], fewer polymer chains attached on the surface of the particles. As consequence, the drastic thermal expansion of the matrix beyond the melting point of HDPE easily broke the network provided by spherical fillers. Meanwhile, also because of the spherical morphology, the low-structure CB aggregates had a stronger capability of movement and reaggregation in the polymer melt. It was clear enough to explain the effect of the CB structure on the network formation and revolution by this model.

CONCLUSIONS

In this study, we investigated the influence of the CB structure on the network formation and evolution in polyethylene/CB composites by electrical and rheological measurements. Phenomenally, the electrical percolation and $m_{cG'}$ of the composite containing high-structure CB was lower compared to the composite containing low-structure CB. This could be explained by the difference between the morphologies of the CB primary aggregates. BP2000 aggregates with a multibranched structure built an effective network more easily in the polymer matrix. However, for the VXC-72 and VXC-68 aggregates, characterized by linear and spheroidal morphologies, it was more difficult to build up an effective and steady network. The relationship between CB fractal structure and nonlinear behavior (Payne effect) of composites was also discussed. It seemed that a tight filler–filler or filler–polymer network could be built by the high-structure CB in the polymer matrix, and this corresponded a lower v value. For the HDPE/VXC-72 and HDPE/VXC-68 composites, weak filler–filler and filler–polymer interactions resulted

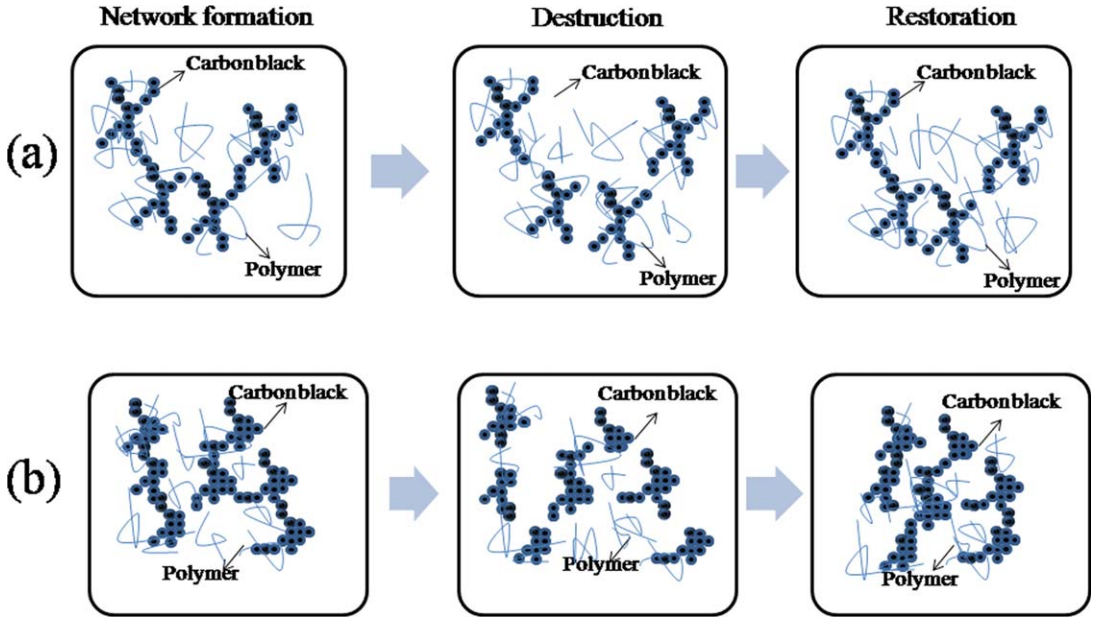

Figure 9. Evolution of the CB aggregate networks in the composite melts: (a) high-structure and (b) low-structure CB. [Color figure can be viewed in the online issue, which is available at wileyonlinelibrary.com.]

in high v values. Simultaneous rheological and conductive measurement is a good way to study the agglomeration kinetics in the polymer melts. In our study, we concentrated on the network evolution during annealing in the rheometer. The phenomenon of the R' decrease and G' increase gave us a clue for understanding the processes of network evolution in the polymer melt. More importantly, we could conjecture the network relaxation behavior from the normal force value.

In summary, for the high-structure CB with a branched morphology, filler–polymer or filler–filler network were easier to form than for the low-structure CB with spherical morphology. The high-structure CB network was more stable with a large strain compared to the low-structure one. Meanwhile, the low-structure CB aggregates had a stronger capability of movement and reaggregation in the polymer melt. This study will be very helpful for us in the design of electrical functional materials, such as positive-temperature-coefficient materials, which are based on network destruction in polymer melts.

ACKNOWLEDGMENTS

This research was supported by the National Natural Science Foundation of China (contract grant number 51103087). The authors acknowledge Chao Liang Zhang (West China College of Stomatology, Sichuan University) for the SEM observations.

REFERENCES

1. Cao, Q.; Song, Y. H.; Tan, Y. Q.; Zheng, Q. *Polymer* **2009**, *50*, 6350.
2. Cao, Q.; Song, Y. H.; Tan, Y. Q.; Zheng, Q. *Carbon* **2010**, *48*, 4268.
3. Konishi, Y.; Cakmak, M. *Polymer* **2006**, *47*, 5371.
4. Huang, S. L.; Liu, Z. Y.; Yin, C. L.; Wang, Y.; Gao, Y. L.; Chen, C.; Yang, M. B. *Colloid Polym. Sci.* **2011**, *289*, 673.
5. Huang, S. L.; Liu, Z. Y.; Yin, C. L.; Wang, Y.; Gao, Y. L.; Chen, C.; Yang, M. B. *Colloid Polym. Sci.* **2011**, *289*, 1927.
6. Mallette, J. G.; Quej, L. M.; Marquez, A.; Manero, O. *J. Appl. Polym. Sci.* **2001**, *81*, 562.
7. Probst, N.; Grivei, E. *Carbon* **2002**, *40*, 201.
8. Rahaman, M.; Chaki, T. K.; Khastgir, D. *J. Mater. Sci.* **2011**, *46*, 3989.
9. Fathi, A.; Hatami, K.; Grady, B. P. *Polym. Eng. Sci.* **2012**, *52*, 549.
10. Huang, J. C. *Adv. Polym. Technol.* **2002**, *21*, 299.
11. Du, F.; Scogna, R. C.; Zhou, W.; Brand, S.; Fischer, J. E.; Winey, K. I. *Macromolecules* **2004**, *37*, 9048.
12. Morozov, I.; Lauke, B.; Heinrich, G. *Comput. Mater. Sci.* **2010**, *47*, 817.
13. Meier, J. G.; Klüppel, M. *Macromol. Mater. Eng.* **2008**, *293*, 12.
14. Schlea, M. R.; Meree, C. E.; Gerhardt, R. A.; Mintz. E. A.; Shofner, M. L. *Polymer* **2012**, *53*, 1020.
15. Huang, S. L.; Liu, Z. Y.; Yin, C. L.; Wang, Y.; Gao, Y. L.; Chen, C.; Yang, M. B. *Macromol. Mater. Eng.* **2012**, *297*, 51.
16. Alig, I.; Skipa, T.; Lellinger, D.; Pötschke, P. *Polymer* **2008**, *49*, 3524.
17. Skipa, T.; Lellinger, D.; Böhm, W.; Saphiannikova, M.; Alig, I. *Polymer* **2010**, *51*, 201.
18. Ren, D. Q.; Zheng, S. D.; Huang, S. L.; Liu, Z. Y.; Yang, M. B. *J. Appl. Polym. Sci.* **2013**, *125*, 3382.
19. Balberg, I. *Carbon* **2002**, *40*, 139.
20. Fernández, M.; Landa, M.; Muñoz, M. E.; Santamaría, A. *Eur. Polym. J.* **2011**, *47*, 2078.
21. Fan, Z.; Advani, S. G. *J. Rheol.* **2007**, *51*, 585.
22. Pötschke, P.; Abder-Goad, M.; Alig, I.; Dudkin, S.; Lellinger, D. *Polymer* **2004**, *45*, 8863.
23. Chae, D. W.; Hong, S. M. *Macromol. Res.* **2011**, *19*, 326.
24. Wu, G.; Song, Y. H.; Zheng, Q.; Du, M.; Zheng, P. J. *J. Appl. Polym. Sci.* **2006**, *88*, 160.
25. Wu, G.; Song, Y. H.; Zheng, Q.; Du, M.; Zheng, P. *J. Polymer* **2006**, *47*, 2442.
26. Romani, F.; Corrieri, R.; Braga, V.; Ciardelli, F. *Polymer* **2002**, *43*, 1115.
27. Bahloul, W.; Legaré, V. B.; David, L.; Cassgnau, P. *J. Polym. Sci. Part B: Polym. Phys.* **2010**, *48*, 1213.
28. Rueb, C. J.; Zukoski, C. F. *J. Rheol.* **1997**, *41*, 197.
29. Sternstein, S.; Zhu, A. *J. Macromolecules* **2002**, *35*, 7262.
30. Zhu, A. J.; Sternstein, S. S. *Compos. Sci. Technol.* **2003**, *63*, 113.
31. Cassagnau, P.; Mélis, F. *Polymer* **2003**, *44*, 6607.
32. Cassagnau, P. *Polymer* **2003**, *44*, 2455.
33. Cassagnau, P. *Polymer* **2008**, *49*, 2183.
34. Miyasaka, K.; Watanabe, K.; Jojima, E.; Aida, H.; Sumita, M.; Ishikawa, K. *J. Mater. Sci.* **1982**, *17*, 1610.
35. Sumita, M.; Asai, S.; Miyadera, N.; Miyasaka, K. *Colloid Polym. Sci.* **1986**, *264*, 212.
36. Meier, J. G.; Mani, J. W.; Klüppel, M. *Phys. Rev. B* **2007**, *75*, 054202.
37. Xu, D. H.; Wang, Z. G. *Macromolecules* **2008**, *41*, 815.
38. Xu, L.; Nakajima, H.; Manias, E.; Krishnamoorti, R. *Macromolecules* **2009**, *42*, 3795.